Hepatic Radiofrequency Ablation–induced Stimulation of Distant Tumor Growth Is Suppressed by c-Met Inhibition[1]

Muneeb Ahmed, MD
Gaurav Kumar, PhD
Marwan Moussa, MD
Yuanguo Wang, PhD
Nir Rozenblum, PhD
Eithan Galun, MD, PhD
S. Nahum Goldberg, MD

Purpose: To elucidate how hepatic radiofrequency (RF) ablation affects distant extrahepatic tumor growth by means of two key molecular pathways.

Materials and Methods: Rats were used in this institutional animal care and use committee–approved study. First, the effect of hepatic RF ablation on distant subcutaneous in situ R3230 and MATBIII breast tumors was evaluated. Animals were randomly assigned to standardized RF ablation, sham procedure, or no treatment. Tumor growth rate was measured for 3½ to 7 days. Then, tissue was harvested for Ki-67 proliferative indexes and CD34 microvascular density. Second, hepatic RF ablation was performed for hepatocyte growth factor (HGF), vascular endothelial growth factor (VEGF), and c-Met receptor expression measurement in periablational rim, serum, and distant tumor 24 hours to 7 days after ablation. Third, hepatic RF ablation was combined with either a c-Met inhibitor (PHA-665752) or VEGF receptor inhibitor (semaxanib) and compared with sham or drug alone arms to assess distant tumor growth and growth factor levels. Finally, hepatic RF ablation was performed in rats with c-Met–negative R3230 tumors for comparison with the native c-Met–positive line. Tumor size and immunohistochemical quantification at day 0 and at sacrifice were compared with analysis of variance and the two-tailed Student *t* test. Tumor growth curves before and after treatment were analyzed with linear regression analysis to determine mean slopes of pre- and posttreatment growth curves on a per-tumor basis and were compared with analysis of variance and paired two-tailed *t* tests.

Results: After RF ablation of normal liver, distant R3230 tumors were substantially larger at 7 days compared with tumors treated with the sham procedure and untreated tumors, with higher growth rates and tumor cell proliferation. Similar findings were observed in MATBIII tumors. Hepatic RF ablation predominantly increased periablational and serum HGF and downstream distant tumor VEGF levels. Compared with RF ablation alone, RF ablation combined with adjuvant PHA-665752 or semaxanib reduced distant tumor growth, proliferation, and microvascular density. For c-Met–negative tumors, hepatic RF ablation did not increase distant tumor growth, proliferation, or microvascular density compared with sham treatment.

Conclusion: RF ablation of normal liver can stimulate distant subcutaneous tumor growth mediated by HGF/c-Met pathway and VEGF activation. This effect was not observed in c-Met–negative tumors and can be blocked with adjuvant c-Met and VEGF inhibitors.

[1] From the Laboratory for Minimally Invasive Tumor Therapies, Department of Radiology, Beth Israel Deaconess Medical Center/Harvard Medical School, 1 Deaconess Rd, WCC 308-B, Boston, MA 02215 (M.A., G.K., M.M., Y.W., S.N.G.); and Goldyne Savad Institute of Gene Therapy (N.R., E.G.) and Division of Image-guided Therapy and Interventional Oncology, Department of Radiology (S.N.G.), Hadassah Hebrew University Hospital, Jerusalem, Israel. Received January 11, 2015; revision requested March 26; revision received June 23; accepted July 7; final version accepted July 21. Supported by the Harvard Medical Faculty Physicians Radiology Foundation, Radiological Society of North America Research Seed Grant (RSD#1215), and Israel Research Foundation/Israel Ministry of Health. **Address correspondence to** M.A. (e-mail: *mahmed@bidmc.harvard.edu*).

Thermal ablation with use of radiofrequency (RF) energy (RF ablation) is now commonly used to treat focal primary hepatocellular carcinoma (HCC) and metastatic liver tumors, including those from primary colorectal and breast cancers (1–3). Therapeutic benefit has been established for many patients, including recent long-term results for the treatment of smaller tumors that approach those of surgical resection in some cases (1,3). However, there is increasing clinical and experimental evidence that RF ablation may, in fact, also induce tumor initiation, growth, and propagation (1,4,5). Several studies suggest that RF ablation may, under unclear clinical circumstances and owing to poorly characterized mechanisms, stimulate growth in residual incompletely treated and viable tumor surrounding the ablation zone for at least some tumor types (eg, HCC or renal cell carcinoma) (4,6,7).

One potential factor that has been implicated in inducing additional tumor growth after RF ablation has been the reactions produced in the normal liver that surrounds the targeted tumors (ie, the red zone beyond the ablative margin of treated normal parenchyma) (5,8). Thus, to further understand potential off-target tumorigenic effects after RF ablation, reactive tissue responses have been studied in the periablational rim surrounding the RF ablation zone, both in residual incompletely treated tumor at the ablative margin and in normal tissue surrounding the ablation zone. Increases in the expression of heat shock proteins, upregulation of proangiogenic factors (eg, hypoxia-inducible factor-1α and vascular endothelial growth factor [VEGF]), and the production of cytokine have all been described (4,9–12). Recently, Rozenblum et al (5) demonstrated that RF ablation of even a small amount of normal liver (3%) can activate the hepatocyte growth factor (HGF)/c-Met kinase pathway by means of α–smooth muscle actin–positive activated myofibroblast recruitment, which has been associated with cancer proliferation and aggressive metastatic invasion in HCC, among others (5,13,14). They also observed increased tumorigenicity after hepatic RF ablation in MDR2 knockout mice, which, because of their chronic liver inflammation, are predisposed to HCC formation (5). However, to our knowledge, the extent that RF ablation stimulates growth of tumor foci outside of the primary treatment organ remains unclear, and the potential mechanistic role of upregulation of the HGF/c-Met pathway (and its known stimulation of downstream VEGF-mediated angiogenesis) has yet to be adequately explored. In addition, as successful clinical ablation necessitates treatment beyond the margins of tumor to include 5–10 mm of normal, uninvolved liver in every case, a greater understanding of secondary reactions with use of models in which normal, nontumor liver tissue is ablated are essential (15).

Therefore, the purpose of our study was to determine *(a)* the effect of RF ablation of normal liver parenchyma on distant tumor growth in two models of in situ breast adenocarcinoma, *(b)* whether RF ablation increases c-Met, HGF, and VEGF in the periablational liver tissue or distant tumor, *(c)* whether adjuvant administration of a c-Met kinase inhibitor (PHA-665752; Tocris, Bristol, England) or a VEGF receptor inhibitor (semaxanib [SU-5416; R&D Systems, Minneapolis, Minn]) can be used to suppress RF-induced stimulation of distant tumor growth in these models, and *(d)* whether RF ablation of

Advances in Knowledge

- Radiofrequency (RF) ablation of normal liver can stimulate distant extrahepatic subcutaneous tumor growth, tumor cell proliferation, and angiogenesis in c-Met–positive tumor lines.
- "Off-target" pro-oncogenic effects of hepatic RF ablation on distant tumor are mediated by increased activation of the hepatocyte growth factor/c-Met pathway locally and within distant c-Met–positive tumors and by downstream vascular endothelial growth factor (VEGF) activation in distant tumors.
- Adjuvant inhibitors of c-Met or VEGF receptors administered in a short window after hepatic RF ablation can block unwanted off-target pro-oncogenic effects on distant extrahepatic c-Met–positive tumor.

Implications for Patient Care

- RF ablation of normal liver, which is required for successful ablation in all clinical cases to achieve a mandatory ablative margin, may incite off-target tumor stimulation in some tumor types.
- RF ablation–induced off-target tumorigenic effects on c-Met–positive tumors can potentially be blocked by using available c-Met or VEGF inhibitors given over a short duration (0–7 days) from the time of ablation.
- Tumor receptor positivity may be used as a biomarker to predict which tumors may be more susceptible to cytokinetic responses produced as a result of hepatic ablation.

Published online before print
10.1148/radiol.2015150080 **Content codes:** GI IR

Radiology 2016; 279:103–117

Abbreviations:
HCC = hepatocellular carcinoma
HGF = hepatocyte growth factor
RF = radiofrequency
VEGF = vascular endothelial growth factor

Author contributions:
Guarantors of integrity of entire study, M.A., G.K.; study concepts/study design or data acquisition or data analysis/interpretation, all authors; manuscript drafting or manuscript revision for important intellectual content, all authors; manuscript final version approval, all authors; agrees to ensure any questions related to the work are appropriately resolved, all authors; literature research, M.A., G.K., M.M., S.N.G.; clinical studies, G.K.; experimental studies, M.A., G.K., M.M., Y.W., N.R., S.N.G.; statistical analysis, M.A., G.K., S.N.G.; and manuscript editing, M.A., G.K., M.M., E.G., S.N.G.

Funding:
This research was supported by the National Institutes of Health (grant CCNE 1U54CA151881-01).

Conflicts of interest are listed at the end of this article.

normal liver would result in similar off-target effects in a subcutaneous c-Met–negative breast tumor model.

Materials and Methods

Overview of Experimental Design

All portions of our study were approved by the institutional animal care and use committee. A total of 197 female Fisher 344 rats (Charles River, Wilmington, Mass) were used. Our study was performed in four parts.

First, RF ablation of normal liver was performed to simulate the standard clinical end point of ablating a margin of normal liver on distant tumors, and R3230 and MATBIII rat adenocarcinoma lines implanted in situ in the mammary fat pad were evaluated (seven rats per arm × two arms per tumor model × two tumor models, n = 28). For R3230 tumors, an additional control arm of no surgical intervention (ie, no treatment) was also performed (n = 5, total = 33). Tumor growth was measured at specified intervals (once per day for R3230 tumors and twice daily for MATBIII tumors), and once tumors reached diameters of 10–11 mm (R3230) or 19–20 mm (MATBIII), animals were randomly assigned (seven per group) to receive either RF ablation alone (21-gauge electrode, 1-cm active tip, application for 5 minutes at a mean tip temperature [±standard deviation] of 70°C ± 2) by means of laparotomy or a sham or control procedure (laparotomy followed by electrode placement without energy application). Tumor growth was measured for seven data points (daily for R3230, twice daily for MATBIII) on the basis of the baseline rate of growth per anticipated time for controls to reach tumor sizes mandating euthanasia. This was followed by sacrifice and harvesting of tissue from the treated liver and distant tumor. The primary outcome was the evaluation of tumor growth (tumor size and growth curve analysis comparisons) with immunohistochemical evaluation for tumor proliferation (Ki-67) and microvascular density (with CD34 staining).

Second, characterization of changes in key growth factor (HGF and VEGF) levels was performed in the periablational rim, serum, and distant tumor. Expression of the c-Met receptor in the periablational rim and distant tumor was also assessed. Animals were implanted with R3230 tumors and randomly assigned to receive standardized RF ablation to normal liver or sham treatment (three animals per arm, n = 6). Animals were sacrificed 3 days after treatment on the basis of previous studies demonstrating peak α–smooth muscle actin–positive activated myofibroblast cell accumulation in the periablational rim and their known HGF production (5). Treated liver and distant tumor tissues were harvested for Western blot analysis of c-Met expression. Additional animals with subcutaneous R3230 tumors were randomly assigned to receive standardized RF ablation to normal liver or sham treatment and sacrificed at 24 hours, 3 days, and 7 days after treatment, with treated liver and distant tumor tissues harvested for immunohistochemical staining for c-Met expression (three per arm × two treatment groups × three time points, n = 18). Liver, serum, and distant tumor HGF and VEGF levels were quantified with enzyme-linked immunosorbent assay 3 days after ablation.

Third, the effect of an adjuvant small-molecule c-Met receptor inhibitor (PHA-665752, subsequently referred to as PHA [16]) or small-molecule VEGF receptor (subtypes 1 and 2) inhibitor (semaxanib or SU5146) (17–19) on distant tumor growth stimulation after RF ablation was studied. PHA was selected on the basis of recent studies demonstrating its efficacy in the suppression of tumorigenesis in a small-animal model of cirrhosis (5). The drug was given after RF ablation of normal liver for both tumor models (R3230 and MATBIII). Experiments were performed as described for the above studies. A total of 44 animals were used (R3230 model: six per arm × four treatment groups; MATBIII model: five per arm × four treatment groups). Animals were randomized to receive either standardized RF ablation or the sham procedure followed by adjuvant intraperitoneal PHA (dose, 0.83 mg/kg; volume, 1 mL) on the third interval measurement (day 3 for R3230 or day 1½ for MATBIII). In addition, the effect of PHA administration timing (0–5 days) after hepatic ablation was also studied in R3230 subcutaneous tumors (six animals per arm × four arms, n = 24). Next, semaxanib was administered after RF ablation of normal liver (intraperitoneally, 8 mg/kg, 3 days after RF ablation), compared with RF ablation of normal liver alone (five per arm × four arms, n = 20). In total, 124 animals were sacrificed at two different time points (3 days and 7 days) for HGF and VEGF quantification, tumor growth measurements, and immunohistochemical evaluation as described earlier.

Finally, a c-Met receptor–negative version of the R3230 breast adenocarcinoma cell lines was established in in vitro cell culture by using sequential exposure to high doses of PHA, with confirmation of c-Met–negative status achieved by using Western blot assays. Animals implanted with subcutaneous c-Met receptor–negative R3230 tumors were randomized to receive standardized RF ablation of normal liver or sham treatment. Tumor growth before and after treatment was performed as described earlier, and animals were sacrificed at 3 days and 7 days after treatment for c-Met quantification and evaluation of proliferation markers and microvascular density. Sixteen animals were used (four per arm × two arms × two time points).

Animal Tumor Models

For all experiments and procedures, anesthesia was induced with intraperitoneal injection of a mixture of ketamine (50 mg/kg; Ketaject [Phoenix Pharmaceutical, St Joseph, Mo]) and xylazine (5 mg/kg; Bayer, Shawnee Mission, Kan). Animals were sacrificed with an overdose of carbon dioxide by using a chamber system (SMARTBOX CO2 chamber system; EZ Systems, Palmer, Pa). All experiments were performed by individuals with experience in performing tumor implantation, RF ablation, and surgery in these models (M.A., G.K., M.M., Y.W., with 15, 3, 5, and 2 years of experience, respectively). All data were verified by the senior author (M.A.).

Initial experiments were performed in a well-characterized R3230 mammary adenocarcinoma model with known and well-established tumor growth rates (20–22). For these studies, the cell line was implanted in female Fisher 344 rats with a mean weight (±standard deviation) of 150 g ± 20 (age, 14–16 weeks) (23). Tumor implantation, evaluation, and preparation were performed as previously described (23). Briefly, one tumor was implanted into each animal by slowly injecting 0.3–0.4 mL of tumor suspension into the mammary fat pad of each animal via an 18-gauge needle. A c-Met receptor–negative version of our R3230 breast adenocarcinoma cell lines was established in in vitro cell culture. Briefly, R3230 adenocarcinoma cells were maintained in Rosewell Park Memorial Institute, or RPMI, media supplemented with fetal bovine serum. Tumor cells were treated with different concentrations of PHA (0.5, 1, 3.3, and 10 μmol/L). R3230 cells (>50%) survived up to PHA concentrations of 3.3 μmol/L and were maintained successively for five generations (treated with PHA every generation). After five generations, cells were tested for c-Met positivity with Western blot assay. A second subcutaneous MATBIII tumor line was established by using similar tumor implantation techniques. Tumors were measured every 1–2 days until they reached 6–7 mm for R3230 and 9–10 mm for MATBIII tumors, at which point they were included in studies.

RF Application

Conventional monopolar RF ablation was applied by using a 500-kHz RF ablation generator (model 3E; Radionics, Burlington, Mass), as previously described (23). Briefly, the 1-cm tip of a 21-gauge electrically insulated electrode (SMK electrode; Cosman Medical, Burlington, Mass) was placed in the liver. RF was applied for 5 minutes with generator output titrated to maintain a designated tip temperature (mean, 70°C ± 2). This standardized method of RF application has been demonstrated previously to provide reproducible coagulation volumes with use of this conventional RF ablation system (23,24). To complete the RF circuit, the animal was placed on a standardized metallic grounding pad (Radionics).

Drug Administration

A c-Met inhibitor, PHA, was obtained in powder form and mixed in 0.9% NaCl to achieve a dose of 0.83 gm/kg. One milliliter (per 200 g animal) was administered by means of intraperitoneal injection at the specified time. A VEGF receptor (subtypes 1 and 2) inhibitor, semaxanib, was obtained in powder form and mixed in dimethyl sulfoxide to achieve a dose of 8 mg/kg. Semaxanib (200 μL) was administered with intraperitornal injection 15 minutes after RF ablation.

Quantification of c-Met, VEGF, and HGF

c-Met quantification was performed by using Western blot analysis. Liver tissue was homogenized by using cell lysis buffer. Briefly, protein was quantified by using a bichinchoninic acid method (Sigma-Aldrich, St Louis, Mo), and 60 μg of total protein was loaded on 10% sodium dodecyl sulfate–polyacrylamide gels and blotted onto nitrocellulose membranes. Nonspecific binding was blocked with 5% (wt/vol) skim milk powder in phosphate-buffered saline with Tween-20 (Cell Signaling Technology, Danvers, Mass) for 1 hour followed by incubation with c-Met 1:100 (45 kDa [SC-162; Santa Cruz Biotechnology, Dallas, Tex]) antibody overnight at 4°C. The membrane was then incubated with appropriate anti-rabbit secondary antibodies followed by radiographic detection. Band intensities were quantified with densitometry by using software (ImageJ 1.3; National Institutes of Health, Bethesda, Md). Standardization of protein amount by using β-actin was also performed. Positive controls were also tested for all assays by using A431 cells with known c-Met positivity. Baseline tumor cells for both R3230 and MATBIII lines were c-Met positive.

Serum and tissue levels of HGF (rat/MHG00, R&D Systems) and VEGF (rat/RRV00 Quantikine kit, R&D Systems) were determined by using an enzyme-linked immunosorbent assay kit according to manufacturer's instructions. Briefly, flash-frozen liver tissue was homogenized in a cold lysis buffer (Cell Signaling Technology, Beverly, Mass) consisting of a 0.1% proteinase inhibitor (Sigma-Aldrich). The homogenates were then centrifuged at 14000 rpm for 20 minutes at 4°C, and the total protein concentration was determined by using bichinchoninic acid. Undiluted serum was used. HGF and VEGF values were then normalized to protein concentration. All samples and standards were measured in duplicate, and the average value was recorded in picograms per milliliter (25,26). All experiments were performed by individuals with experience in performing these assays (M.A., G.K., M.M., and Y.W., with 3–15 years of experience). All data were verified by the senior author (M.A.).

Tumor Growth Measurements

Tumors were measured in both longitudinal and transverse diameters by using mechanical calipers (G.K. and M.M., with 3 years of experience), and an average diameter was calculated (20). Tumors reaching mean sizes of 6–7 mm were measured at five discrete intervals, either daily for R3230 tumors or twice daily for MATBIII tumors, to determine a temporal pretreatment growth rate. The timing of measurement was different for the two different tumor lines as MATBIII tumors demonstrated a much faster growth rate. Once tumors reached target mean diameters of 10–11 mm (R3230) or 19–20 mm (MATBIII), they were randomly allocated to specified treatment arms. After RF ablation or sham treatment, measurements were obtained for seven intervals (again, daily for R3230 and twice daily for MATBIII tumors). Mean starting tumor size was similar for all comparative treatment groups at initial evaluation and at randomization and/or treatment time.

Tissue Harvesting

Animals were sacrificed at specified times as outlined earlier. The primary site of liver ablation was harvested and sliced perpendicularly to the direction of electrode insertion (11,23). Distant

tumors were also harvested and sliced. All samples were fixed in 10% formalin overnight at 4°C, embedded in paraffin, and sliced at a thickness of 5 μm. Tissues were stained with hematoxylin and eosin for gross pathologic examination.

Immunohistochemical Staining

Sections from distant tumors were prepared and immunohistochemical staining was used to evaluate cell proliferation (percentage of Ki-67–positive cells) as previously described (11). Specimen slides were imaged and analyzed by using a microscope (Micromaster I; Fisher Scientific, Pittsburgh, Pa) and software (Micron Imaging; Westover Scientific, Mill Creek, Wash). Five random high-power fields were analyzed for a minimum of three specimens for each parameter and scored in a blinded fashion to remove observer bias. For Ki-67 (Ab16667; Abcam, Cambridge, Mass), the percentage of positive cells (a ratio of stained and unstained cells) was calculated for each field and averaged for each specimen. For c-Met staining (SC-162), rim thickness and percentage cell positivity were recorded by using methods previously described for other proteins upregulated in the periablational rim (11,12). Staining for CD34 (an endothelial cell marker [Ab8158, Abcam]) and quantification of microvascular density were performed as previously described (27). As an additional control to ensure uniformity of staining, whenever direct comparisons were made immunohistochemical examination was repeated with all relevant comparison slides stained at the same time. All experiments were performed by individuals with 3–15 years of experience in performing immunohistochemistry (M.A., G.K., M.M., and Y.W.). All data were verified by the senior author (M.A.).

Statistical Analysis

Software (SPSS 13.0; SPSS, Chicago, Ill) was used for statistical analysis. All data are given as means ± standard deviations. Selected (day 0 and at the time of sacrifice) mean tumor sizes and immunohistochemical quantification were compared with analysis of variance, with testing including a posttreatment interaction term. Additional posthoc analysis was performed with a two-sample, two-tailed Student *t* test if, and only if, the results of analysis of variance achieved statistical significance. $P < .05$ was considered indicative of a statistically significant difference. Tumor growth curves before and after treatment were analyzed with linear regression analysis models to determine the slope of the pre- and posttreatment growth curve on a per-tumor basis. From these data, mean posttreatment growth curve slopes were calculated and compared by using analysis of variance and paired two-tailed *t* tests.

Results

Effect of RF Ablation of Normal Liver on Distant Subcutaneous Tumor Growth

Starting tumor size and tumor growth rates were the same for all groups in all studies (Table 1, not significant for all comparisons). No difference in tumor growth rate or end tumor diameter was observed when comparing the sham treatment arm and the control tumor arm ($P = .92$) (Fig 1a). Yet, a significantly greater R3230 tumor growth rate was observed after RF ablation of normal liver such that tumors were significantly larger at 7 days compared with those of sham-treated or control animals (mean diameter, 17.0 mm ± 2.1 vs 13.7 mm ± 0.9 and 13.8 mm ± 0.8, respectively; $P < .02$), which represents an increase in tumor size of 34.8% ± 0.1 versus 13.7% ± 0.1 ($P < .001$) (Table 1, Fig 1a). In addition, RF ablation of normal liver significantly increased the rate of R3230 tumor growth compared with that before treatment (slope: 0.51 ± 0.14 [$R^2 = 0.91 \pm 0.06$] before ablation vs 0.83 ± 0.27 [$R^2 = 0.97 \pm 0.02$] after ablation; $P = .018$) (Table 1) and that after sham treatment (slope: 0.32 ± 0.13 [$R^2 = 0.92 \pm 0.06$], $P < .001$) (Table 1). Concordantly, R3230 tumors at 7 days after RF ablation demonstrated significantly greater cellular proliferation (percentage of Ki-67– positive cells per high-power field) compared with that after sham treatment (82.7% ± 4.5 vs 25.0% ± 3.0, respectively; $P < .001$). Finally, increased microvascular density was also observed in distant tumors in animals treated with liver RF ablation compared with the sham procedure (number of vessels per high-power field: 50.9 ± 15.9 vs 25.1 ± 8.1, respectively; $P = .003$).

Similar findings were observed with RF ablation of normal liver for the confirmatory MATBIII tumor model (Fig 1b). RF ablation of normal liver resulted in faster tumor growth rates in distant MATBIII tumors such that at 3½ days after ablation, tumors in the RF ablation arm measured 24.4 mm ± 2.5 compared with 21.9 mm ± 1.2 ($P = .01$) (Table 1). Likewise, there was significantly increased tumor cellular proliferation in animals treated with hepatic RF ablation compared with sham treatment (percentage of Ki-67–positive cells: 75.8% ± 1.8 vs 57.5% ± 7.7, respectively; $P = .02$). Again, microvascular density within the distant tumor was also greater in the liver RF ablation group compared with the sham group (49.9 vessels per high-power field ± 7.3 vs 32.8 vessels per high-power field ± 7.9, respectively; $P = .002$).

Effect of Hepatic RF Ablation on HGF and VEGF Levels in the Periablational Rim, Serum, and Distant Intratumoral Tissue

Compared with sham treatment, hepatic RF ablation increased HGF levels in the periablational liver (28745 pg/mL ± 2530 vs 19801 pg/mL ± 2781, $P < .01$), serum (27036 pg/mL ± 625 vs 17814 pg/mL ± 329, $P < .001$ both comparisons), and distant R3230 tumor tissue (15469 pg/mL ± 485 vs 14354 pg/mL ± 426, $P < .05$) at 72 hours after treatment (Fig 2a). Similarly, increased VEGF levels were observed after hepatic RF ablation compared with sham treatment in the periablational rim (3759 pg/mL ± 201 vs 1547 pg/mL ± 165, $P < .001$) and distant tumor tissue (63967 pg/mL ± 1243 vs 43407 pg/mL ± 9352, $P < .01$) at 72 hours after treatment (Fig 2b, $P < .02$). The serum VEGF level for either RF ablation or sham treatment was not detectable at 72 hours. HGF was increased to the

Table 1

Summary of Subcutaneous Tumor Growth and Proliferative Index for Different Organs and Tumor Models

Treatment Arm	End Diameter (mm)	Change in Diameter after Treatment (mm)	Growth Curve Slope		Percentage of Ki-67–Positive Cells	Microvascular Density (cells per high-power field)
			Before RF Ablation	After RF Ablation		
Hepatic RF ablation alone vs sham on distant tumor growth						
R3230						
Sham	13.7 ± 0.9	5.3 ± 0.8	0.63 ± 0.12	0.34 ± 0.14	24.7 ± 3.6	25.1 ± 8.1
RF ablation	17.1 ± 2.2*	9.0 ± 1.8*	0.61 ± 0.08	0.88 ± 0.25*	70.1 ± 8.6*	50.9 ± 15.9*
MATBIII						
Sham	21.9 ± 1.2	11.4 ± 1.5	1.83 ± 0.21	0.39 ± 0.20	57.5 ± 7.7	32.8 ± 7.9
RF ablation	24.4 ± 2.5*	14.7 ± 2.1*	1.86 ± 0.44	0.77 ± 0.20*	75.8 ± 1.8*	49.9 ± 7.3*
PHA without or with hepatic RF ablation on distant tumor growth						
R3230						
RF ablation + PHA	12.8 ± 1.5*	5.3 ± 1.3*	0.62 ± 0.17*	0.19 ± 0.08*	23.3 ± 3.2*	22.5 ± 0.2*
PHA alone	14.7 ± 2.9	6.8 ± 1.6	0.60 ± 0.2	0.52 ± 0.16	25.6 ± 3.5	39.5 ± 6.9
MATBIII						
RF ablation + PHA	22.5 ± 0.5*	12.1 ± 1.1*	1.94 ± 0.31	0.36 ± 0.09*	48.7 ± 3.9*	25.1 ± 2.6*
PHA alone	24.5 ± 0.6	14.0 ± 0.4	1.88 ± 0.10	0.80 ± 0.15	62.7 ± 5.9	36.2 ± 1.1
Semaxanib without or with hepatic RF ablation on distant tumor growth†						
RF ablation + semaxanib	16.4 ± 0.9*	7.6 ± 1.2*	0.69 ± 0.21	0.53 ± 0.10*	27.5 ± 1.7*	16.0 ± 3.0*
Semaxanib alone	15.2 ± 0.6	6.7 ± 1.0	0.70 ± 0.08	0.48 ± 0.17	31.6 ± 0.8	29.2 ± 7.6

Note.—Data are means ± standard deviations.

* $P < .05$ when compared with sham group.

† Performed only with R3230 tumors.

greatest degree in the periablational liver tissues (45.2% increase from that with sham treatment) and in the serum (51.2% increase), whereas greatest increases in VEGF expression after liver RF ablation were observed in distant tumor (47.4% increase) (Fig 2).

Effect of Hepatic RF Ablation on Local Periablational and Distant Intratumoral c-Met Expression

For R3230, localized increased c-Met expression was observed at immunohistochemical staining in a geographic rim surrounding the liver RF ablation zone, which was similar at 24 hours (percentage positive cells per high-power field: 54.9% ± 3.2) and 72 hours (percentage positive cells per high-power field: 55.1% ± 7.2) after RF ablation and greater than that in either adjacent unablated liver or liver from the sham treatment group (Fig 3a, 3b). Confirmatory Western blot analysis demonstrated that RF ablation of normal liver results in increased c-Met protein expression in tissue immediately surrounding the periablational rim at 3 days after RF ablation compared with sham treatment (20.3% vs 12.6% of peak densitometry, respectively) (Fig 3c). This locally increased hepatic c-Met expression in the periablational rim was similar for all arms treated with hepatic RF ablation, regardless of whether the animal had distant tumor implanted (Fig 3d). Furthermore, no elevated c-Met expression was observed with either sham procedure or untreated control arms or in untreated liver beyond the ablation zone. C-Met protein levels were also elevated in distant R3230 tumor after liver ablation compared with sham treatment (15.1% vs 11.2% of peak densitometry, respectively).

Effect of Adjuvant Inhibitors on RF Ablation–induced Stimulation of Distant Tumor Growth

With the addition of adjuvant PHA, distant tumor growth rates after RF ablation of normal liver decreased so that the tumor size at 7 days (mean, 12.8 mm ± 1.5) was equivalent to that in the sham group ($P = .15$) and smaller than that in the group that received RF ablation alone ($P < .001$) (Table 1, Fig 4a). Similarly, a significant decrease in tumor cell proliferation was observed at 7 days for the group that received RF ablation and PHA (percentage of Ki-67–positive cells: 23.4% ± 3.2) to baseline levels ($P = .45$ vs sham; $P < .001$ vs RF ablation) (Table 1). In animals treated with sham procedure and PHA alone,

Figure 1

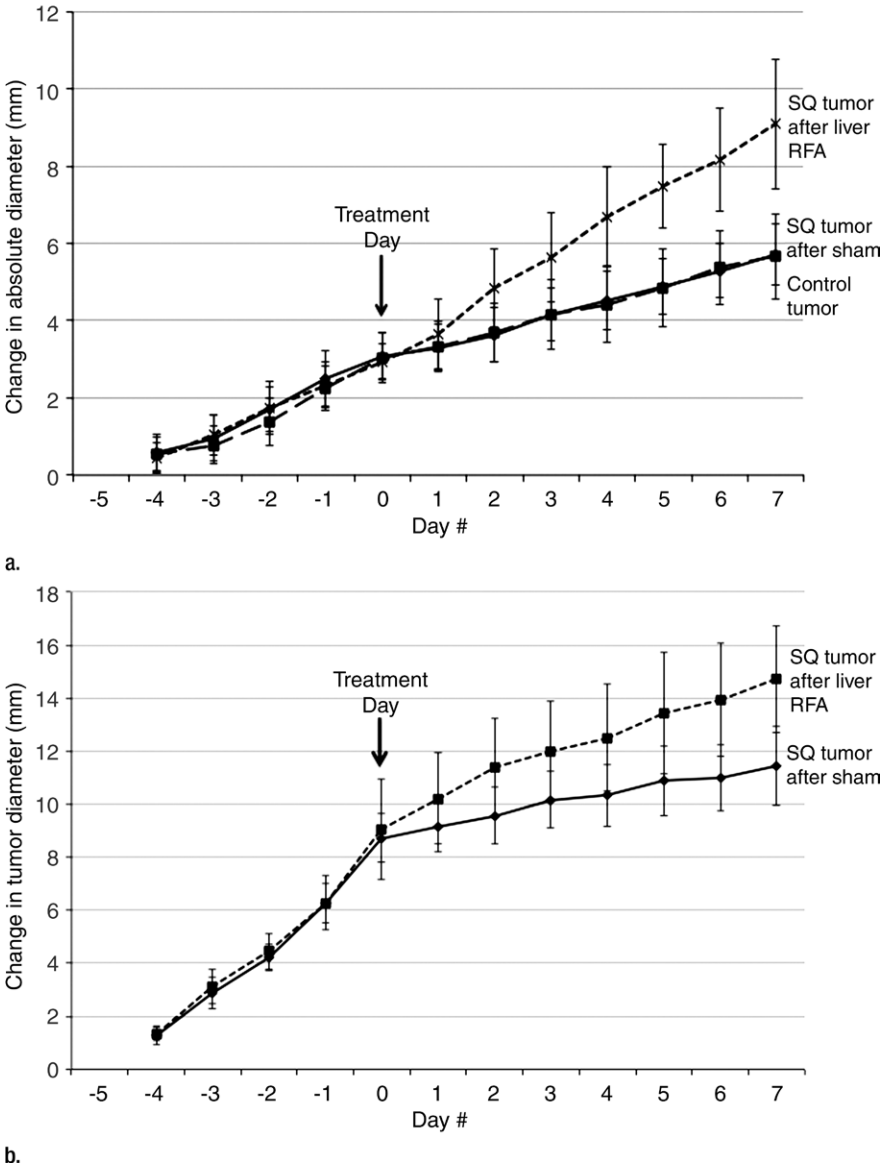

Figure 1: Graphs show that RF ablation (*RFA*) of normal liver increases growth of distant subcutaneous tumors compared with sham treatment. *SQ* = subcutaneous. **(a)** Curves for R3230 tumors demonstrate same rate of growth for all groups before treatment. After hepatic RF ablation (day 0), growth rate of distant tumors is significantly greater at 7 days such that end tumor diameter is significantly greater than that with sham treatment ($P < .01$). **(b)** Curves for MATBIII tumors show that hepatic RF ablation at day 0 stimulated distant subcutaneous tumor growth such that end tumor diameter 3½ days after ablation was significantly greater than that with sham treatment ($P = .001$).

tumor sizes and proliferative indexes were similar to that in the sham group. A maximum reduction in tumor size at 7 days was observed for animals treated with RF ablation followed by adjuvant single-dose PHA given at 3 days after RF ablation compared with PHA given immediately after RF ablation (0 days) or at 5 days after RF ablation (mean tumor size: 14.9 mm ± 1.1 at day 0, 12.8 mm ± 1.5 at day 3, and 17.2 mm ± 1.0 at day 5; $P < .02$ for all comparisons). Adjuvant PHA similarly reduced MATBIII tumor growth rates, tumor diameter at 7 days after RF ablation, and tumor cell proliferation compared with sham treatment (P = not significant) (Table 1). Reductions in microvascular density to baseline (sham) levels were also observed in distant tumors when adjuvant PHA was administered with RF ablation for R3230 and MATBIII tumor models after hepatic RF ablation (Table 1).

Combined liver RF ablation with post–RF ablation adjuvant PHA treatment on day 3 reduced c-Met expression in the periablational rim compared with RF ablation alone (rim thickness at 24 hours: 727.6 μm ± 61.2 with RF ablation and 316.6 μm ± 26.6 with RF ablation and PHA; rim thickness at 72 hours: 728.0 μm ± 34.2 with RF ablation and 505.9 μm ± 68.7 with RF ablation and PHA; $P < .01$ for all comparisons) and percentage positive cells per high-power field (24 hours: 54.9% ± 3.2 with RF ablation and 34.6% ± 5.4 with RF ablation and PHA; 72 hours: 55.1% ± 7.2 with RF ablation and 19.4% ± 2.9 with RF ablation and PHA; $P < .05$ for all comparisons). At Western blot analysis, adjuvant PHA given 3 days after liver RF ablation reduced c-Met protein levels to baseline (sham) levels in the periablational rim of liver tissue (RF ablation and PHA: 12.6% of peak; RF ablation: 20.3% of peak; sham treatment: 12.6% of peak) and in the distant R3230 tumor (RF ablation and PHA: 11.8% of peak; RF ablation: 15.1% of peak; sham treatment: 11.2% of peak) (Fig 3c). Adjuvant PHA on day 3 significantly reduced post–RF ablation serum increases in HGF back to baseline levels (RF ablation and PHA: 16212 pg/mL ± 161; RF ablation: 27036 pg/mL ± 625; $P < .01$).

Adjuvant semaxanib administered 3 days after hepatic RF ablation reduced distant tumor growth back to at least baseline sham levels at 7 days after treatment compared with RF ablation alone (7.6 mm ± 1.2 vs 10.5 mm ± 1, respectively $P = .01$) and versus sham (6.0 mm ± 0.5, $P = .07$) (Table 1, Fig 4b). Tumor growth and diameter at 7 days after treatment were similar

Figure 2

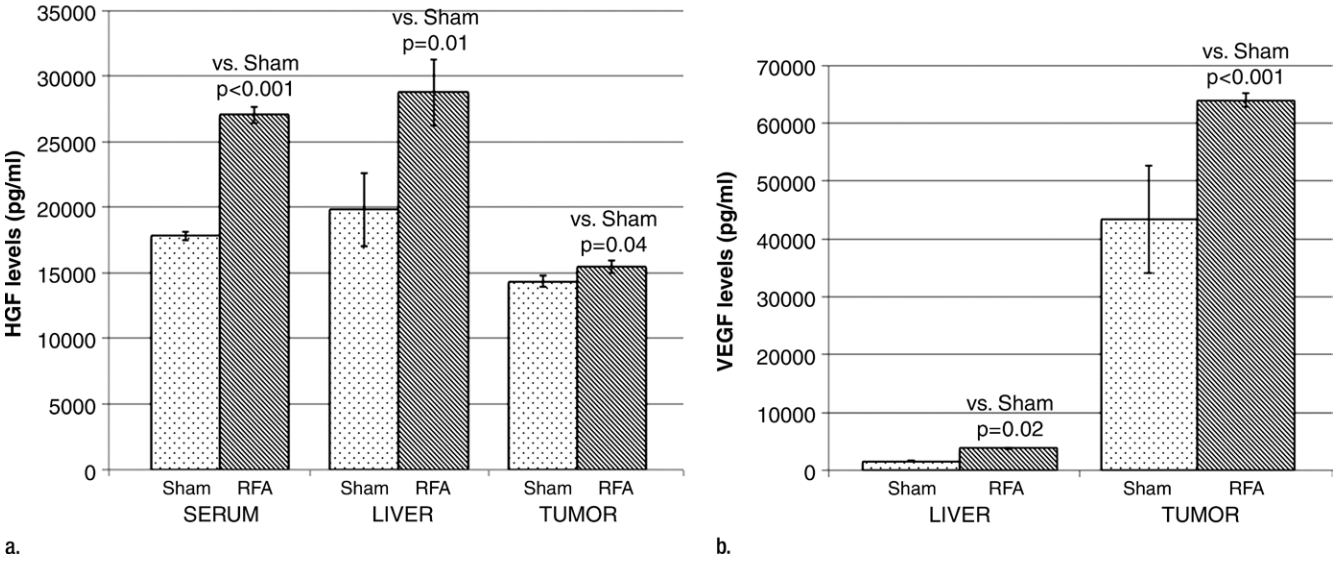

Figure 2: Bar graphs show effects of hepatic RF ablation *(RFA)* on local, serologic, and distant R3230 tumor HGF and VEGF levels obtained 72 hours after RF ablation with enzyme-linked immunosorbent assay. **(a)** Hepatic RF ablation increased local periablational and serum HGF levels to greatest degree compared with sham treatment (and to a much lesser degree in distant R3230 tumor). **(b)** In comparison, hepatic RF ablation led to significant increases in distant tumor VEGF levels and only a marginal increase in periablational VEGF levels. Serum VEGF levels were undetectable for both arms (not shown).

between semaxanib alone and the sham arms (P = not significant). Similarly, hepatic RF ablation and semaxanib reduced distant tumor proliferation and microvascular density back to baseline sham levels (Table 1) ($P < .001$ vs RF ablation for both end points). Semaxanib and RF ablation reduced periablational liver and distant tumor VEGF levels back to baseline sham levels, which were lower than those with either RF ablation alone or RF ablation and PHA arms (Table 2, $P < .001$). Similarly, semaxanib and RF ablation treatment reduced HGF levels in the periablational liver, serum, and distant tumor to levels significantly lower than those in hepatic RF ablation, RF ablation and PHA, or sham arms ($P < .001$).

Effect of RF Ablation of Normal Liver on Growth in Distant Subcutaneous c-Met–Negative R3230 Tumors

c-Met–negative R3230 tumors demonstrated slower tumor growth rates compared with c-Met–positive R3230 tumors as the mean time to reach 10–11 mm was 6 days ± 1 and 18 days ± 1, respectively ($P < .01$). Hepatic RF ablation did not result in an increase in distant tumor growth rate or significant change in tumor diameter at 7 days after treatment compared with sham treatment (tumor diameter: 17.2 mm ± 0.5 vs 17.2 mm± 0.3, respectively, $P = .999$; change in diameter after procedure: 10.0 mm ± 0.2 vs 10.1 mm ± 0, $P = .35$) (Fig 5). In addition, distant tumor proliferation (percentage of Ki-67–positive cells) and microvascular density (representing VEGF-mediated angiogenesis) were the same for both RF and sham treatment arms (percentage of Ki-67–positive cells: 19.3% ± 2.7 vs 19.5% ± 2.1, respectively, $P = .93$; microvascular density: 32.7 vessels per high-power field ± 2.1 vs 31 vessels per high-power field ± 2.0, $P = .66$). In addition, no increase in distant tumor c-Met expression was observed for hepatic RF ablation compared with sham treatment at Western blot analysis (Fig 5).

Discussion

Several studies suggest that RF ablation can stimulate aggressive tumor biology—manifested as increased tumor incidence, metastatic or invasive behavior, and overall tumor growth—in incompletely ablated tumor or in separate sites of tumor within the liver even when only apparently normal liver has been ablated. For example, incomplete RF ablation of intrahepatic tumors can stimulate tumor cell growth in the partially injured residual cells in the periablational rim or in intrahepatic and/or intraorgan tumor foci separate from the ablation site (4,7,28). In the treatment of early solitary HCC, Lencioni et al (1) reported an excellent long-term local tumor control of 90% but observed likely substantially higher rates of new visible tumors at 5 years than might be expected from such populations that have not undergone hepatic RF ablation (80% vs 25%–45% reported elsewhere) (29). More recently, Rozenblum et al (5) demonstrated increased growth in multiple de novo intrahepatic HCC tumor foci after ablation of small volumes of liver (<3% of overall liver) in an MDR2 knockout model of cirrhosis. However, the literature largely focuses on the intrahepatic effects of liver tumor ablation, whereas off-target effects of hepatic ablation (particularly from

Figure 3

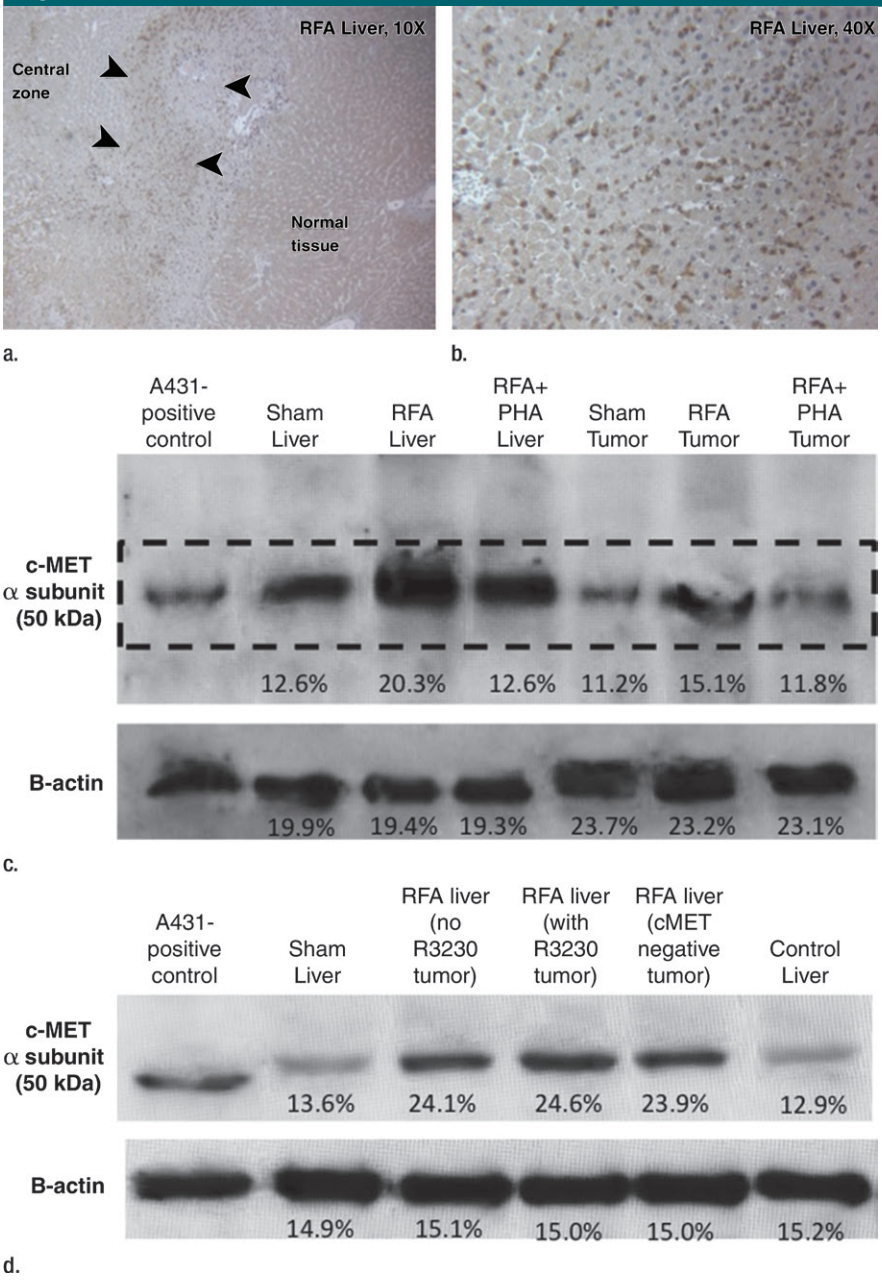

Figure 3: Hepatic RF ablation *(RFA)* increases periablational and distant tumor c-Met receptor expression. **(a, b)** c-Met expression is increased in periablational rim in normal liver after RF ablation compared with sham treatment. Immunohistochemical staining for c-Met receptor expression demonstrates a rim of increased c-Met staining around ablation zone (arrowheads) after RF ablation of normal liver. No changes were observed at site of sham treatment (ie, electrode placement in liver). **(c)** Liver RF ablation–induced changes in local and distant c-Met without and with PHA. Western blot assays demonstrate increased c-Met receptor protein in tissue harvested from periablational tissue surrounding liver ablation zone compared with sham treatment (seen as dense bands after gel electrophoresis at 50-kDa level, where c-Met receptor α subunit is expected, after β-actin standardization) (20.3% vs 12.6%, respectively). c-Met receptor protein levels are also slightly increased in distant tumor after hepatic RF ablation compared with sham treatment (15.1% vs 11.2%, respectively). β-actin levels were similar for all arms, which confirms increases in observed c-Met receptor expression. **(d)** Liver RF ablation–induced changes in local c-Met with and without implanted distant c-Met–positive or negative tumor. Western blot assays demonstrate increased periablational c-Met expression after hepatic RF ablation in all arms, regardless of whether there was any distant tumor present (24.1% vs 24.6%) or whether distant tumor expressed the c-Met receptor (24.6% vs 23.9%).

the mandatory ablation of normal tissue necessary in nearly all clinical cases to achieve an effective periablational margin) on distant extrahepatic tumor growth remains poorly characterized to our knowledge. Indeed, previous reports of pro-oncogenic effects of liver ablation have been based on models where incomplete ablation of liver tumors was performed, and off-target pro-oncogenic effects were attributed to secondary reactions within the partially injured tumor cells (4,10,28,30). Thus, much of the previous literature does not directly address the very common clinical scenario of complete local ablation, where normal liver in an adequate ablative margin comprises approximately 75% of ablated tissue volume (31,32).

In our study, RF ablation of normal liver parenchyma stimulated growth of distant breast tumors implanted in the mammary fat pad with correlative increases in tumor proliferation and angiogenesis. By ablating normal liver tissue, we confirmed that the response of liver tissue to nonlethal hyperthermic injury is also a key driver of unwanted protumorigenic effects. Furthermore, as these results were reproducible for two separate tumor lines, such off-target pro-oncogenic effects after hepatic RF ablation may be wide ranging. As the standard clinical end point in widespread practice is to ablate the entire tumor (either primary HCC or liver metastasis) and up to a 5–10 mm circumferential margin of normal parenchymal tissue around the ablation zone, this is potentially highly clinically relevant (15,33,34). Therefore, for cases

of locally successful hepatic RF tumor ablation, the potential for stimulation of tumor foci elsewhere in the body exists. Accordingly, further study is required to identify those factors that place particular tumor types and patients at risk for ablation-induced tumor progression.

As a next step, we observed upregulation of the HGF/c-Met pathway and VEGF after hepatic RF ablation, both of which have known roles in driving tumor growth, metastatic invasion, and aggressive tumor biology (16,35,36). On the basis of our results, we hypothesize several steps in the pathway underlying how local tissue reactions surrounding hepatic RF ablation can lead to distant effects of increased tumor growth. First, the increased local HGF and c-Met activation from liver RF ablation incites a local positive feedback loop, further increasing local HGF production and c-Met expression (as has been described previously [37]), leading to markedly elevated levels in the periablational rim that was subsequently blocked by c-Met inhibition. Next, HGF is released into the serum (leading to the observed elevated levels after RF ablation), circulates to distant tumor, and binds intratumoral c-Met receptors. Finally, activation of c-Met receptors results in downstream increased intratumoral VEGF expression and VEGF-mediated angiogenesis both in the periablational rim and in distant tumor. These findings are in keeping with the known relationship between HGF activation of the c-Met receptor and downstream increased VEGF expression and the fact that we observed no elevation of VEGF in the serum after RF ablation despite seeing such increases in the liver and tumor (38). This hypothesis is further strengthened by our studies of hepatic RF ablation in a c-Met–negative clone of the same tumor line, where no accelerated growth, c-Met expression, or angiogenesis was observed in distant tumors.

We further demonstrated that activated cytokinetic pathways contributing to off-target tumor stimulation can be successfully blocked by combining hepatic RF ablation with adjuvant drugs against key receptor targets. Here, a c-Met inhibitor administered as a single dose after hepatic RF ablation can successfully suppress RF ablation–induced distant tumor growth, tumor cell proliferation, and angiogenesis. We separately showed that targeting a VEGF receptor with semaxanib (a VEGF receptor subtype 1 and 2 inhibitor) can also block off-target RF ablation–induced tumor stimulation. Both agents, tested separately to target specific mediators in a common pathway, were equally effective in these short-term studies. This may suggest that blocking different targets in the pathway may be sufficient in suppressing pro-oncogenic effects. However, even when a primary pathway, such as HGF/c-Met or VEGF, is a significant driver of tumor growth and proliferation and can be successfully targeted with adjuvant pharmacologic inhibition, there is a known benefit to targeting parallel pathways to achieve a more durable treatment response (39,40). For example, epidermal growth factor receptor activation has been linked to early failure of c-Met inhibition in the treatment of lung cancer (41). Other growth factors and cytokines that have been identified as drivers of tumor growth (including hypoxia-inducible factor-1α and interleukin-6) are also upregulated after RF ablation (4,42). Several of these are linked with c-Met activation through shared downstream mediators or direct involvement in the c-Met pathway (43). In particular, c-Met is closely linked to both neoangiogenesis through stimulation of endothelial cells and VEGF production and hypoxia through hypoxia-inducible factor-1α–dependent increases in Met expression (44,45). Therefore, additional study to target these pathways may be beneficial, especially in tumor lines that demonstrate no response or a partial response to initial HGF/c-Met inhibition. Many multikinase small-molecule inhibitors that are currently available or in active development block multiple receptor targets (including semaxanib, which also has a weak affinity for the c-Met receptor [46]) and therefore may be very effective in suppressing off-target pro-oncogenic effects of RF ablation. Regardless, further clinical development of this drug ablation combination therapy paradigm will require testing the many agents that are in active clinical use to determine which have greatest efficacy.

Our results further highlight that the development of optimal combination therapy paradigms will ultimately depend on several different factors. Successful targeting of key mediators of a pathway that starts in one organ and ends in another distant site, or where there may be unwanted effects from the same factors both locally and systemically, likely requires tailoring the adjuvant drug delivery and pharmacokinetics to a specific time and location (ie, periablational tissue or distant tumor) and time. For example, we originally chose to administer adjuvant PHA 3 days after RF ablation for most of our studies on the basis of previous studies that demonstrated peak activated myofibroblast recruitment to the periablational rim (8). In our study, varying the timing of drug administration between 0 and 5 days after RF ablation supports this selection and highlights the relatively narrow window of administration temporally associated with the RF ablation. Adjuvant PHA administered at days 0 or 3 resulted in either prevention of increased tumor growth or an immediate reduction in tumor growth rate to baseline levels, compared with a much reduced effect when administered 5 days after RF ablation. Separately, the optimal site or sites of pharmacologic action also must be tailored to specific targets. Here, PHA was likely acting in both the periablational rim, where adjuvant PHA blocked the HGF/c-Met–positive feedback loop and suppressed periablational HGF levels, and potentially at the distant tumor, where despite persistently high circulating levels of HGF, the RF ablation–induced growth stimulation was blocked. Conversely, the VEGF receptor inhibitor semaxanib likely acted predominantly in the distant tumor, where VEGF levels were markedly elevated after hepatic RF ablation, and to a much lesser degree in the periablational rim. Thus, understanding when and where contributing mediators are upregulated after

Figure 4

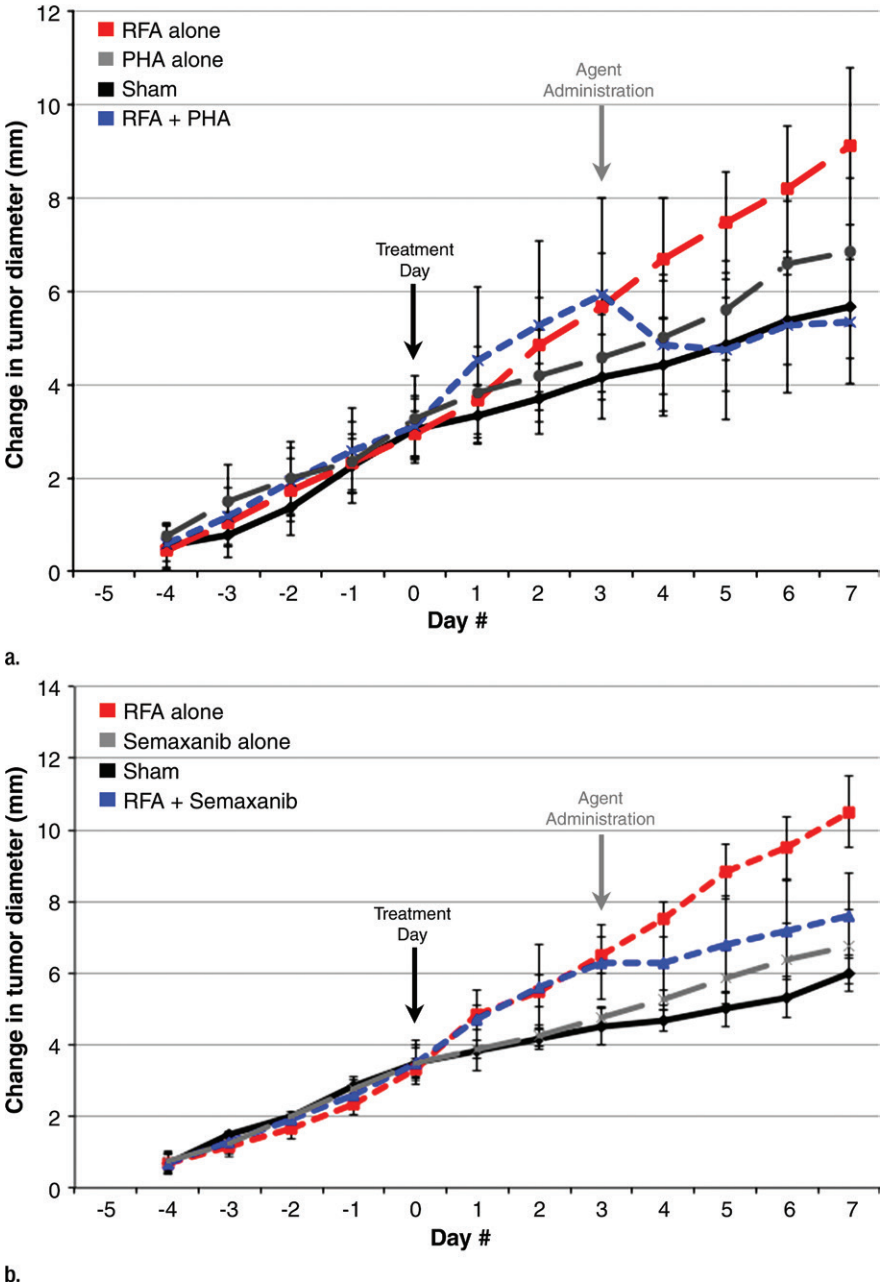

Figure 4: Adjuvant c-Met and VEGF receptor inhibitors block hepatic RF ablation *(RFA)*–induced distant tumor growth. **(a)** Effect of liver RF ablation on distant tumor growth in R3230 adenocarcinoma cell line with suppression with c-Met kinase inhibitor. Graph shows that adjuvant PHA given 3 days after hepatic RF ablation decreases distant R3230 tumor growth rate back to baseline compared with RF ablation alone. PHA alone treatment arm has same growth rate as sham arm (which indicates that c-Met inhibitor does not have active effect on tumor growth by itself). **(b)** Effect of liver RF ablation on distant tumor growth in R3230 adenocarcinoma cell line with suppression of VEGF receptor inhibitor (semaxanib). Similar to PHA, adjuvant semaxanib blocks hepatic RF ablation–induced stimulation of distant R3230 tumor growth back to baseline compared to that with hepatic RF ablation alone.

hepatic RF ablation is crucial when using adjuvant drugs to successfully block unwanted effects.

Finally, we demonstrated that positivity of the c-Met receptor in an otherwise similar tumor model is associated with susceptibility to off-target effects of hepatic RF ablation. This suggests that only some tumors with certain receptors will be susceptible to RF ablation–induced tumorigenicity and may partly account for why others have reported antitumor immunity (ie, the so-called "abscopal" effects) for other tumor types after liver ablation (47). Along these lines, identification of key responsible molecular pathways may form the basis for testing for tumor biomarkers (eg, c-Met) that could play an important role in the prospective identification of those patients or tumors that are "at risk" and therefore may benefit from adjuvant therapy after ablation, an approach now commonly used in the treatment of many cancers. Along the same lines, Poon et al (48) demonstrated that preablation serum VEGF levels may be used to identify subsets of patients with HCC who have poorer outcomes after hepatic RF ablation. Given the known heterogeneity of c-Met receptor positivity in HCC (49), the development of such biomarkers will be essential for selecting patients who will have greater benefit from ablation or, conversely, will require adjuvant therapy to suppress unwanted effects. Furthermore, as we have demonstrated with HGF levels after hepatic RF ablation combined with an adjuvant c-Met inhibitor, changes in serologic levels of key downstream markers may present an opportunity for developing postintervention tests that can help predict response to adjuvant therapy.

We acknowledge that, given the wide array of mechanistic responses reported after thermal ablation, several other elements likely contributed to this pro-oncogenic post-RF pathway, or at the very least may be involved in parallel pathways. This is further supported by the fact that adjuvant c-Met inhibition (upstream in the pathway) only partially reduced downstream intratumoral

Table 2

Summary of Changes in Serum, Liver, and Distant Tumor HGF and VEGF Levels for Hepatic RF Ablation without and with Adjuvant Drug Therapies

	Serum		Liver		Tumor	
Treatment Group	HGF (pg/mL)	VEGF (pg/mL)*	HGF (pg/mL)	VEGF (pg/mL)	HGF (pg/mL)	VEGF (pg/mL)
Sham	17814 ± 329	ND	19801 ± 2781	1547 ± 165	14354 ± 426	43407 ± 9352
RF ablation	27036 ± 625 ($P < .001$ vs sham)	ND	28745 ± 2530 ($P = .01$ vs sham)	3759 ± 201 ($P < .001$ vs sham)	15469 ± 485 ($P = .04$ vs sham)	63967 ± 1243 ($P = .02$ vs sham)
RF ablation + PHA	16212 ± 161 ($P = .001$ vs sham; $P < .001$ vs RF ablation)	ND	27971 ± 1106 ($P = .009$ vs sham; $P = .65$ vs RF ablation)	2184 ± 182 ($P = .01$ vs sham; $P < .001$ vs RF ablation)	13077 ± 662 ($P = .04$ vs sham; $P = .007$ vs RF ablation)	60347 ± 1305 ($P = .03$ vs sham; $P = .02$ vs RF ablation)
RF ablation + semaxanib	2453 ± 199 ($P < .001$ vs sham; $P < .001$ vs RF ablation)	ND	5582 ± 52 ($P < .001$ vs sham; $P < .001$ vs RF ablation)	777 ± 129 ($P = .003$ vs sham; $P < .001$ vs RF ablation)	10855 ± 147 ($P < .001$ vs sham; $P < .001$ vs RF ablation)	45327 ± 1501 ($P = .74$ vs sham; $P < .001$ vs RF ablation)

Note.—Data are means ± standard deviations.

* ND = values were not detected.

VEGF, which suggests parallel activation of other mechanisms. Early (6–24 hours) increased interleukin-6 production has been reported after hepatic ablation (8,50), and interleukin-6 has well-described effects on downstream activation of the HGF/c-Met pathway (51). Others have described increased PI3 K and Akt activation, which may be interlinked or occurring in parallel to HGF/c-Met activation (52). In addition, although pharmacologic suppression of c-Met expression was effective in this tumor cell line, use of more specific techniques (eg, small interfering RNA suppression) may offer the ability to differentiate key contributors to the mechanistic pathway in future studies (53). Finally, several different cell populations may be the source of various growth factors and cytokines, including inflammatory cells (including macrophages, neutrophils, or activated myofibroblasts) recruited to the periablational rim or native hepatocytes and endothelial cells reacting to hyperthermic injury, as these have been reported to excrete or be under the influence of HGF, VEGF, and related cytokines. Thus, characterization of additional key contributors, such as specific cytokines and/or cell populations, may offer additional insight into how and when such off-target effects occur.

There are several limitations of our study that indicate many additional points worthy of investigation. As noted earlier, further characterization in a wider range of tumor lines and types, including the use of models with intrahepatic tumors, is warranted, particularly to characterize the effects of different tumors and microenvironments. However, we note that many tumor types have been shown to express high levels of the c-Met receptor, and c-Met inhibition has been successfully used to suppress RF ablation–induced intrahepatic HCC tumor growth as well (5), which suggests a wider applicability of our findings to tumor models with high rates of c-Met expression. Similarly, the tumor lines studied do not normally demonstrate early or widespread metastases after implantation, and further study on the effect of hepatic RF ablation on the promotion of aggressive tumor behavior such as c-Met– and VEGF-mediated vascular invasion or the promotion of new distant metastases is required. In addition, although we observed 30%–40% increases in distant tumor size in a relatively early and short window (range, 0–7 days) after RF ablation, evaluation of longer times after ablation is likely warranted, particularly to study durability of response to adjuvant drugs with RF ablation and to identify upregulation of potential "escape" pathways that might lead to more aggressive tumor biology at a later time. Additional studies in tumor models with variable and smaller tumor sizes would also be helpful in determining if off-target prooncogenic effects of hepatic RF ablation exhibit certain threshold effects. Furthermore, although our study has used RF ablation of normal liver as its primary model, tumor ablation is performed by using multiple different energy sources (eg, microwave, laser, ultrasound, irreversible electroporation, and cryoablation) and in many different organ sites (eg, kidney, lung, adrenal, bone, soft tissue). Thus, additional studies are required to determine whether effects reported herein are present in other clinically relevant situations. Finally, PHA is a very effective c-Met inhibitor molecule, and the degree to which other clinically available c-Met pathway inhibitors are able to block RF ablation–induced tumor growth stimulation, and the level of inhibition (eg, direct receptor binding vs HGF antibodies), remain to be seen (36,54). Ultimately, future studies should include confirmation in other tumor types and organ sites of ablation, performing long-term

Figure 5

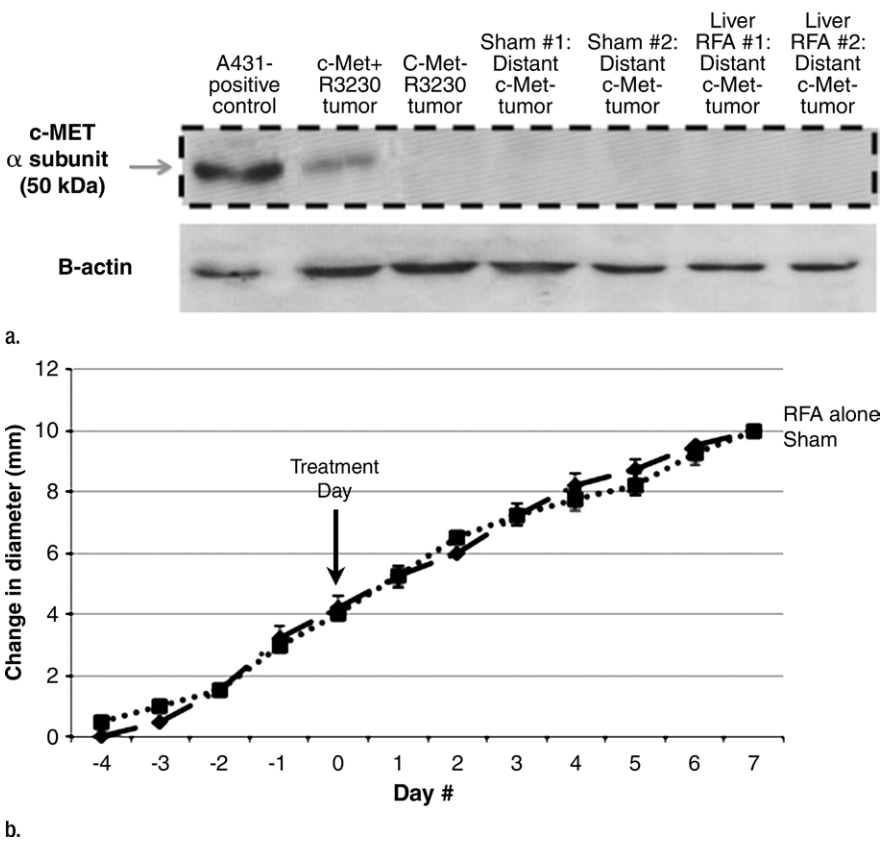

Figure 5: Hepatic RF ablation *(RFA)* does not stimulate distant tumor growth in c-Met–negative R3230 cell line. **(a)** Western blot assays in distant c-Met–negative R3230 tumor samples 7 days after treatment demonstrate no difference in c-Met expression between hepatic RF ablation and sham procedure. **(b)** Graph shows similar growth rates for both arms before treatment (day 0). Hepatic RF ablation does not increase distant c-Met–negative R3230 tumor growth or end tumor diameter (day 7) compared with sham treatment (mean, 17.2 mm ± 0.5 vs 17.2 mm ± 0.3, respectively; $P = .999$).

survival studies, parallel study of potential postablative abscopal effects, and correlation to clinical studies.

In conclusion, RF ablation of normal liver, simulating obtaining complete clinical ablation of a focal tumor by creating an ablative margin, can stimulate distant tumor growth in two c-Met–positive tumor lines (and not in a matched c-Met–negative cell line) driven by a combination of periablational tissue reactions and systemic in-tumor effects that are in part mediated by HGF/c-Met pathway and VEGF and can be blocked with c-Met and VEGF receptor inhibitors given in a short window after ablation. Finally, tumor lines lacking c-Met expression did not respond to off-target effects of hepatic RF ablation, which suggests that the potential use of c-Met tumor receptor positivity as a biomarker requires further study to predict those tumors that may be more susceptible to cytokinetic responses produced as a result of hepatic ablation.

Disclosures of Conflicts of Interest: M.A. disclosed no relevant relationships. **G.K.** disclosed no relevant relationships. **M.M.** disclosed no relevant relationships. **Y.W.** disclosed no relevant relationships. **N.R.**. disclosed no relevant relationships. **E.G.** disclosed no relevant relationships. **S.N.G.** Activities related to the present article: disclosed no relevant relationships. Activities not related to the present article: is a paid consultant for Cosman Company and Angiodynamics; has grants/grants pending from Cosman Company. Other relationships: disclosed no relevant relationships.

References

1. Lencioni R, Cioni D, Crocetti L, et al. Early-stage hepatocellular carcinoma in patients with cirrhosis: long-term results of percutaneous image-guided radiofrequency ablation. Radiology 2005;234(3):961–967.
2. Meloni MF, Andreano A, Laeseke PF, Livraghi T, Sironi S, Lee FT Jr. Breast cancer liver metastases: US-guided percutaneous radiofrequency ablation—intermediate and long-term survival rates. Radiology 2009; 253(3):861–869.
3. Solbiati L, Ahmed M, Cova L, Ierace T, Brioschi M, Goldberg SN. Small liver colorectal metastases treated with percutaneous radiofrequency ablation: local response rate and long-term survival with up to 10-year follow-up. Radiology 2012;265(3):958–968.
4. Nijkamp MW, van der Bilt JD, de Bruijn MT, et al. Accelerated perinecrotic outgrowth of colorectal liver metastases following radiofrequency ablation is a hypoxia-driven phenomenon. Ann Surg 2009;249(5):814–823.
5. Rozenblum N, Zeira E, Scaiewicz V, et al. Oncogenesis: an "off-target" effect of radiofrequency ablation. Radiology DOI: 10.1148/radiol.15141695. Published online March 30, 2015.
6. Kroeze SG, van Melick HH, Nijkamp MW, et al. Incomplete thermal ablation stimulates proliferation of residual renal carcinoma cells in a translational murine model. BJU Int 2012;110(6 Pt B):E281–E286.
7. Shiozawa K, Watanabe M, Takahashi M, Wakui N, Iida K, Sumino Y. Analysis of patients with rapid aggressive tumor progression of hepatocellular carcinoma after percutaneous radiofrequency ablation. Hepatogastroenterology 2009;56(96):1689–1695.
8. Rozenblum N, Zeira E, Bulvik B, et al. Radiofrequency ablation: inflammatory changes in the periablative zone can induce global organ effects, including liver regeneration. Radiology 2015;276(2):416–425.
9. Ahmad F, Gravante G, Bhardwaj N, et al. Changes in interleukin-1β and 6 after hepatic microwave tissue ablation compared with radiofrequency, cryotherapy and surgical resections. Am J Surg 2010;200(4):500–506.
10. Kong J, Kong J, Pan B, et al. Insufficient radiofrequency ablation promotes angiogenesis of residual hepatocellular carcinoma via HIF-1α/VEGFA. PLoS One 2012; 7(5):e37266.
11. Solazzo SA, Ahmed M, Schor-Bardach R, et al. Liposomal doxorubicin increases radiofrequency ablation–induced tumor destruction by increasing cellular oxidative and

nitrative stress and accelerating apoptotic pathways. Radiology 2010;255(1):62–74.

12. Yang W, Ahmed M, Tasawwar B, et al. Radiofrequency ablation combined with liposomal quercetin to increase tumour destruction by modulation of heat shock protein production in a small animal model. Int J Hyperthermia 2011;27(6):527–538.
13. Harun N, Costa P, Christophi C. Tumour growth stimulation following partial hepatectomy in mice is associated with increased upregulation of c-Met. Clin Exp Metastasis 2014;31(1):1–14.
14. Xie B, Xing R, Chen P, et al. Down-regulation of c-Met expression inhibits human HCC cells growth and invasion by RNA interference. J Surg Res 2010;162(2):231–238.
15. Wang X, Sofocleous CT, Erinjeri JP, et al. Margin size is an independent predictor of local tumor progression after ablation of colon cancer liver metastases. Cardiovasc Intervent Radiol 2013;36(1):166–175.
16. Liu X, Newton RC, Scherle PA. Development of c-MET pathway inhibitors. Expert Opin Investig Drugs 2011;20(9):1225–1241.
17. Litz J, Sakuntala Warshamana-Greene G, Sulanke G, Lipson KE, Krystal GW. The multi-targeted kinase inhibitor SU5416 inhibits small cell lung cancer growth and angiogenesis, in part by blocking Kit-mediated VEGF expression. Lung Cancer 2004;46(3):283–291.
18. Mendel DB, Schreck RE, West DC, et al. The angiogenesis inhibitor SU5416 has long-lasting effects on vascular endothelial growth factor receptor phosphorylation and function. Clin Cancer Res 2000;6(12):4848–4858.
19. Ogawara K, Abe S, Un K, Yoshizawa Y, Kimura T, Higaki K. Determinants for in vivo antitumor effect of angiogenesis inhibitor SU5416 formulated in PEGylated emulsion. J Pharm Sci 2014;103(8):2464–2469.
20. D'Ippolito G, Ahmed M, Girnun GD, et al. Percutaneous tumor ablation: reduced tumor growth with combined radio-frequency ablation and liposomal doxorubicin in a rat breast tumor model. Radiology 2003;228(1):112–118.
21. Yang W, Ahmed M, Elian M, et al. Do liposomal apoptotic enhancers increase tumor coagulation and end-point survival in percutaneous radiofrequency ablation of tumors in a rat tumor model? Radiology 2010;257(3):685–696.
22. Yang W, Ahmed M, Tasawwar B, et al. Combination radiofrequency (RF) ablation and IV liposomal heat shock protein suppression: reduced tumor growth and increased animal endpoint survival in a small animal tumor model. J Control Release 2012;160(2):239–244.
23. Ahmed M, Monsky WE, Girnun G, et al. Radiofrequency thermal ablation sharply increases intratumoral liposomal doxorubicin accumulation and tumor coagulation. Cancer Res 2003;63(19):6327–6333.
24. Monsky WL, Kruskal JB, Lukyanov AN, et al. Radio-frequency ablation increases intratumoral liposomal doxorubicin accumulation in a rat breast tumor model. Radiology 2002;224(3):823–829.
25. Abarbanell AM, Wang Y, Herrmann JL, et al. Toll-like receptor 2 mediates mesenchymal stem cell–associated myocardial recovery and VEGF production following acute ischemia-reperfusion injury. Am J Physiol Heart Circ Physiol 2010;298(5):H1529–H1536.
26. Ishii H, Oota I, Takuma T, Inomata K. Developmental expression of vascular endothelial growth factor in the masseter muscle of rats. Arch Oral Biol 2001;46(1):77–82.
27. Hakimé A, Peddi H, Hines-Peralta AU, et al. CT perfusion for determination of pharmacologically mediated blood flow changes in an animal tumor model. Radiology 2007;243(3):712–719.
28. Nikfarjam M, Muralidharan V, Christophi C. Altered growth patterns of colorectal liver metastases after thermal ablation. Surgery 2006;139(1):73–81.
29. Mittal S, El-Serag HB. Epidemiology of hepatocellular carcinoma: consider the population. J Clin Gastroenterol 2013;47(Suppl):S2–S6.
30. Thompson SM, Callstrom MR, Butters KA, et al. Role for putative hepatocellular carcinoma stem cell subpopulations in biological response to incomplete thermal ablation: in vitro and in vivo pilot study. Cardiovasc Intervent Radiol 2014;37(5):1343–1351.
31. Ahmed M, Solbiati L, Brace CL, et al. Image-guided tumor ablation: standardization of terminology and reporting criteria—a 10-year update. Radiology 2014;273(1):241–260.
32. Ke S, Ding XM, Qian XJ, et al. Radiofrequency ablation of hepatocellular carcinoma sized > 3 and ≤ 5 cm: is ablative margin of more than 1 cm justified? World J Gastroenterol 2013;19(42):7389–7398.
33. Anderson EM, Lees WR, Gillams AR. Early indicators of treatment success after percutaneous radiofrequency of pulmonary tumors. Cardiovasc Intervent Radiol 2009;32(3):478–483.
34. Ahmed M, Brace CL, Lee FT Jr, Goldberg SN. Principles of and advances in percutaneous ablation. Radiology 2011;258(2):351–369.
35. Goetsch L, Caussanel V, Corvaia N. Biological significance and targeting of c-Met tyrosine kinase receptor in cancer. Front Biosci (Landmark Ed) 2013;18:454–473.
36. Goyal L, Muzumdar MD, Zhu AX. Targeting the HGF/c-MET pathway in hepatocellular carcinoma. Clin Cancer Res 2013;19(9):2310–2318.
37. Hage C, Rausch V, Giese N, et al. The novel c-Met inhibitor cabozantinib overcomes gemcitabine resistance and stem cell signaling in pancreatic cancer. Cell Death Dis 2013;4:e627.
38. Abounader R, Laterra J. Scatter factor/hepatocyte growth factor in brain tumor growth and angiogenesis. Neuro-oncol 2005;7(4):436–451.
39. Navis AC, Bourgonje A, Wesseling P, et al. Effects of dual targeting of tumor cells and stroma in human glioblastoma xenografts with a tyrosine kinase inhibitor against c-MET and VEGFR2. PLoS One 2013;8(3):e58262.
40. Takeuchi S, Wang W, Li Q, et al. Dual inhibition of Met kinase and angiogenesis to overcome HGF-induced EGFR-TKI resistance in EGFR mutant lung cancer. Am J Pathol 2012;181(3):1034–1043.
41. Landi L, Minuti G, D'Incecco A, Cappuzzo F. Targeting c-MET in the battle against advanced non–small cell lung cancer. Curr Opin Oncol 2013;25(2):130–136.
42. Fifis T, Malcontenti-Wilson C, Amijoyo J, et al. Changes in growth factor levels after thermal ablation in a murine model of colorectal liver metastases. HPB (Oxford) 2011;13(4):246–255.
43. Gherardi E, Birchmeier W, Birchmeier C, Vande Woude G. Targeting MET in cancer: rationale and progress. Nat Rev Cancer 2012;12(2):89–103.
44. Kitajima Y, Ide T, Ohtsuka T, Miyazaki K. Induction of hepatocyte growth factor activator gene expression under hypoxia activates the hepatocyte growth factor/c-Met system via hypoxia inducible factor-1 in pancreatic cancer. Cancer Sci 2008;99(7):1341–1347.
45. Bussolino F, Di Renzo MF, Ziche M, et al. Hepatocyte growth factor is a potent angiogenic factor which stimulates endothelial cell motility and growth. J Cell Biol 1992;119(3):629–641.
46. Wang SY, Chen B, Zhan YQ, et al. SU5416 is a potent inhibitor of hepatocyte growth factor receptor (c-Met) and blocks HGF-induced invasiveness of human HepG2 hepatoma cells. J Hepatol 2004;41(2):267–273.
47. Erös de Bethlenfalva-Hora C, Mertens JC, Piguet AC, et al. Radiofrequency ablation sup-

presses distant tumour growth in a novel rat model of multifocal hepatocellular carcinoma. Clin Sci (Lond) 2014;126(3):243–252.

48. Poon RT, Lau C, Pang R, Ng KK, Yuen J, Fan ST. High serum vascular endothelial growth factor levels predict poor prognosis after radiofrequency ablation of hepatocellular carcinoma: importance of tumor biomarker in ablative therapies. Ann Surg Oncol 2007;14(6):1835–1845.

49. Ang CS, Sun MY, Huitzil-Melendez DF, et al. c-MET and HGF mRNA expression in hepatocellular carcinoma: correlation with clinicopathological features and survival. Anticancer Res 2013;33(8):3241–3245.

50. Erinjeri JP, Thomas CT, Samoilia A, et al. Image-guided thermal ablation of tumors increases the plasma level of interleukin-6 and interleukin-10. J Vasc Interv Radiol 2013; 24(8):1105–1112.

51. Sun R, Jaruga B, Kulkarni S, Sun H, Gao B. IL-6 modulates hepatocyte proliferation via induction of HGF/p21cip1: regulation by SOCS3. Biochem Biophys Res Commun 2005; 338(4):1943–1949.

52. Tulasne D, Foveau B. The shadow of death on the MET tyrosine kinase receptor. Cell Death Differ 2008;15(3):427–434.

53. Ahmed M, Kumar G, Navarro G, et al. Systemic siRNA nanoparticle-based drugs combined with radiofrequency ablation for cancer therapy. PLoS One 2015;10(7):e0128910.

54. Porter J. Small molecule c-Met kinase inhibitors: a review of recent patents. Expert Opin Ther Pat 2010;20(2):159–177.